PHYSICAL REVIEW B **79**, 113101 (2009)

Charge disproportionation in $CaCu_3Fe_4O_{12}$

Xianfeng Hao,[1,2,*] Yuanhui Xu,[1,3] Faming Gao,[1] Defeng Zhou,[3] and Jian Meng[2,†]
[1]*Department of Chemical Engineering, Yanshan University, Qinhuangdao 066004, China*
[2]*Key Laboratory of Rare Earth Chemistry and Physics, Changchun Institute of Applied Chemistry, Chinese Academy of Sciences, Changchun 130022, People's Republic of China*
[3]*School of Biological Engineering, Changchun University of Technology, Changchun 130012, People's Republic of China*

(Received 1 November 2008; revised manuscript received 3 January 2009; published 3 March 2009)

First-principles calculations using the APW+lo method, as implemented in the WIEN2K code, have been used to investigate the structural, electronic, and magnetic properties of the perovskite $CaCu_3Fe_4O_{12}$, including the high-temperature *Im*-3 and low-temperature *Pn*-3 phase. The high-temperature phase presents a homogeneous valence and an orbital degenerate half-metallic behavior, which is consistent with the previous theoretical result. Instead orbital ordering, charge ordering, or disproportionation on Fe sites occur in the low-temperature phase, leading to the insulating character. More importantly, the charge disproportionation is of $2d^5L \rightarrow d^5L^2 + d^5$ type (where L denotes an oxygen hole or a ligand hole), and the origin for the phenomenon is discussed in detail.

DOI: 10.1103/PhysRevB.79.113101 PACS number(s): 71.30.+h, 71.15.Mb, 71.20.−b

Orbital ordering in transition-metal magnetic oxides arises when their transition-metal ions possess an electron configuration with unevenly filled degenerate *d* states and hence Jahn-Teller (JT) instability. In general, this takes the form of a cooperative JT effect when the lattice distorts take place so as to lift the orbital degeneracy. The scenario requires narrow bands and is ubiquitous in transition-metal Mott insulators. On the other hand, upon gradual delocalization of degenerate electrons, the JT distortion and corresponding orbital ordering become less favorable and the orbital degeneracy is lifted via charge ordering (also known as charge disproportionation or charge density wave), e.g., at half of all sites a degenerate level becomes empty and at the others doubly occupied instead of the JT distortion, as exemplified in rare-earth nickelates.[1]

Besides the nickelates mentioned above, the same mechanism seems to be operative in some ferrates that nominally contain Jahn-Teller Fe^{4+} ($t_{2g}^3 e_g^1$) ions but which instead of a JT distortion segregate into Fe^{3+} ($t_{2g}^3 e_g^2$) and Fe^{5+} ($t_{2g}^3 e_g^0$) without orbital degeneracy. Recently, the complex perovskite compound $CaCu_3Fe_4O_{12}$, which is the first Fe^{4+} oxide to be discovered in almost three decades, has been synthesized at pressures above 9 GPa and temperature of around 1300 K. $CaCu_3Fe_4O_{12}$ has been found to undergo an interesting phase transition to a charge disproportionation ferrimagnetic state at 210 K, with the resistivity increasing quickly below this temperature. This charge disproportionation is considered to be the $CaFeO_3$ type ($2Fe^{4+} \rightarrow Fe^{3+} + Fe^{5+}$) and is accompanied by a structural transition (from the high-temperature phase with *Im*-3 space group to the low-temperature phase with *Pn*-3 space group) that leads to the aliovalent ions ordered in the rock-salt pattern.[2] Experimentally, the charge ordering manifests itself in oxygen breathing and in different bond valence sum values on the two Fe sites, e.g., 3.51 and 4.33 for Fe^{3+} and Fe^{5+}, respectively. However, the analysis of x-ray photoemission spectra[3] of $CaFeO_3$ suggested that the charge ordering state results from the charge disproportionation of $2d^5L \rightarrow d^5L^2 + d^5$ rather than $2d^4 \rightarrow d^3 + d^5$ (L: an oxygen hole or a ligand hole). This compound can be viewed as a "valence-bond insulator" with small or negative charge-transfer gap such as has first been suggested for $NaCuO_4$.[4] Hence, further study is needed to settle the issue of Fe valence states in $CaCu_3Fe_4O_{12}$.

In order to better understand the peculiar electronic and magnetic properties of $CaCu_3Fe_4O_{12}$, it is essential to investigate the electronic structures of Fe 3*d* electrons. In this work, we have investigated the valence and spin states of the Fe ions in $CaCu_3Fe_4O_{12}$ by using density-functional theory. The insulator-metal transition and the unusual magnetic structure in $CaCu_3Fe_4O_{12}$ are apparently connected to the charge disproportionation. Therefore, the theoretical calculations that can provide further details about the structural, electronic, and magnetic properties of $CaCu_3Fe_4O_{12}$ and related physical properties therefore are highly desirable, especially with regard to the charge disproportionation.

All calculations reported in this work were carried out using high accurate full-potential linearized augmented plane wave plus local orbitals (FP-LAPW+lo) method[5,6] with density-functional theory implemented in the WIEN2K package.[7,8] In this method, the space is divided into an interstitial region and nonoverlapping muffin-tin (MT) spheres centered at the atomic sites. In the MT region, the basis sets are described by radial solutions of the one-particle Schrödinger equation (at fixed energy) and their energy derivatives are multiplied by spherical harmonics.

In order to achieve energy convergence, the wave functions in the interstitial region were expanded in plane waves with a cutoff of $R_{MT}^{min} K_{max} = 7$, where R_{MT}^{min} denotes the smallest atomic sphere radius and K_{max} gives the magnitude of the largest K vector in the plane-wave expansion. The values of the atomic sphere radii (R_{MT}) were chosen as 2.41, 1.88, 1.92, and 1.67 a.u. for Ca, Cu, Fe, and O, respectively. For electron population analysis, the muffin-tin radii (R_{MT}) were chosen as touching spheres to keep as much core charges inside the muffin-tin sphere as possible. The valence wave functions inside the spheres are expanded up to $l_{max} = 10$, while the charge density was Fourier expanded up to $G_{max} = 14$. The total Brillouin zone was sampled with 2000 k

1098-0121/2009/79(11)/113101(4)

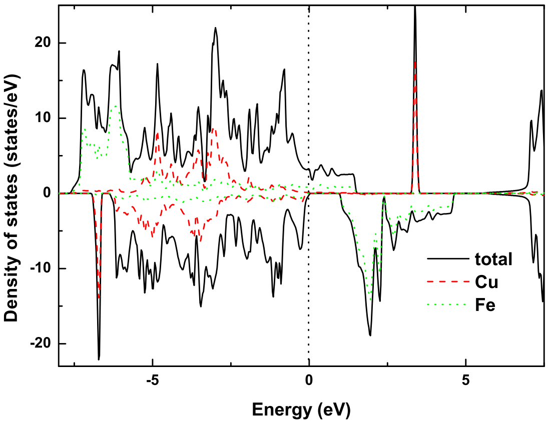

FIG. 1. (Color online) Electronic density of states and projection onto the LAPW Fe and Cu spheres indicating the *d* contributions for $CaCu_3Fe_4O_{12}$ in the high-temperature *Im*-3 phase obtained by GGA+*U* within $U=4.0$ eV for Fe and $U=7.0$ eV for Cu, respectively.

points. The Brillouin zone integration is carried out with a modified tetrahedron method.[9] Self-consistency is considered to be achieved when the total-energy difference between succeeding iterations is less than 10^{-5} Ry/f.u.

As for the exchange-correlation potential, we employed the standard generalized gradient approximation (GGA) using the Perdew-Burke-Ernzerhof scheme.[10] In addition, to properly describe the strong electron correlation in the 3*d* transition-metal oxides, the GGA plus on site repulsion *U* method (GGA+*U*) was used[11–13] with the effective *U* values ($U_{\rm eff}=U-J$) of 2.0–4.0 eV for Fe and 5.0–7.0 eV for Cu, respectively. Unless otherwise indicated, the reported results are for $U_{\rm eff}=4.0$ and 7.0 eV for Fe and Cu, respectively.

In order to clarify the charge disproportionation and valence state of Fe ions in $CaCu_3Fe_4O_{12}$, we first investigated the electronic and magnetic properties within the ferrimagnetic configuration of the high-temperature *Im*-3 phase as a reference. In agreement with the previous computed results,[14] we found that this phase is half-metallic, with the majority spin being metallic with sufficient unfilled states above the Fermi level and the minority spin being semiconducting. Figure 1 represents the total and projected density of states on the Fe 3*d* and Cu 3*d* orbitals in *Im*-3 phase $CaCu_3Fe_4O_{12}$. The octahedral surrounding of Fe atom splits the Fe-*d* manifolds into t_{2g} and e_g levels. In the up-spin channel, the Fe-t_{2g} and Fe-e_g levels are found in the energy range ∼−7.5 eV, extend to 2.0 eV above the Fermi energy, and show a significant mixing with O-*p* states. In the down-spin channel, the Fe-*d* levels lie ∼1.2 eV above the Fermi level. This leads to the conclusion that the oxidation state of Fe is nominally 4+ (d^4:$t_{2g}^{3\uparrow}e_g^{1\uparrow}$), which agree with the Mössbauer spectroscopy and the bond valence sums for Fe (+3.77) based on the experimental data.[2] Due to the antiferromagnetic interaction between the Fe and Cu ions, the spin-down Cu 3*d* states are all occupied while the spin-up Cu 3*d* states occur at around −4 eV with the remaining up-spin Cu 3*d* states above the Fermi level. This feature is consistent with the d^9 ($t_{2g}^{3\downarrow}e_g^{2\downarrow}t_{2g}^{3\uparrow}e_g^{1\uparrow}$) configuration of the Cu^{2+} ion. Partial density of states analysis indicates that the unoccupied up-spin states have mainly the $d_{x^2-y^2}$ orbital character. Our spin-polarized calculations gave a moment of $3.3-3.5\mu_B$ at the Fe site, and the magnetic moment at the Cu site for a MT radius of 1.88 a.u. is found to be -0.2 to $-0.7\mu_B$, which change monotonously when Hubbard *U* is turned on. The calculated magnetic moments for Fe^{4+} and Cu^{2+} ions are less than the expected values of $gS=4\mu_B$ and $gS=1\mu_B$, respectively. The induced moment is found to reside at the O sites, suggesting a considerable charge transfer among the Fe, Cu, and O atoms, i.e., the hybridization interaction among them. The total magnetic moment is $13.0\mu_B$/f.u., which is in agreement with the half-metallic behavior.

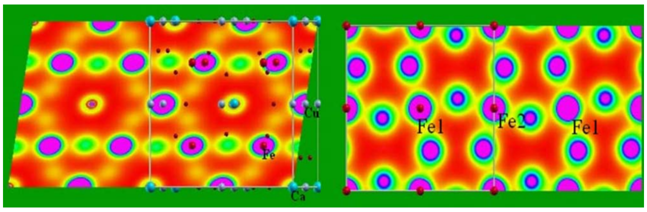

FIG. 2. (Color online) The charge density contour plots in the (110) plane (left) for $CaCu_3Fe_4O_{12}$ in the high-temperature *Im*-3 phase and the charge density contour plots in the (100) plane (right) indicating the charge disproportionation for $CaCu_3Fe_4O_{12}$ in the low-temperature *Pn*-3 phase.

Up to now our analysis has been done based on the electronic structure of the high-temperature *Im*-3 phase, in which there is just one Wyckoff site (8*c*) for the Fe atoms. As shown in Fig. 2, all the Fe ions possess uniform charge density plot. To investigate how the charge disproportionation takes place and to what extent, we have performed similar calculations on the low-temperature *Pn*-3 phase. Structural studies on the low-temperature phase using electron diffraction and synchrotron x-ray powder diffraction revealed the Wyckoff site 8*c* splits into two kinds of Fe sites (4*b* and 4*c*) arranged in the rock-salt pattern, as mentioned above.

In general, the similarity of the crystal structures of the high-temperature and low-temperature phases is well reflected by the similarity of the density of states (shown in Fig. 3). Yet, the differences between the electronic properties of the high-temperature phase and that of the low-temperature phase become much clearer from a detailed analysis of the near-E_F states. The most striking consequence of the structural distortion is the dramatic change near the Fermi surface range. The low-temperature phase is an insulator without density of states across the Fermi level, seen for the high-temperature phase in the majority spin channel. This finding is consistent with the experimental conductivity study.[2]

Figure 4 shows the site-decomposed electronic density of states for the low-temperature *Pn*-3 phase from the GGA+*U* method. It is clear that the Ca atoms have largely denoted their valence electrons to the other constituents and that they themselves entered into nearly pure ionic states (evident from the small number of states in the valence band and a larger number of states in the conduction band). It can be recalled that in the low-temperature *Pn*-3 phase, Fe1

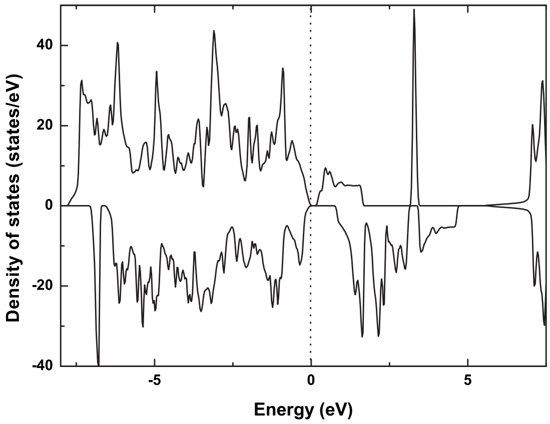

FIG. 3. Electronic density of states for $CaCu_3Fe_4O_{12}$ in the low-temperature Pn-3 phase obtained by GGA+U within U=4.0 eV for Fe and U=7.0 eV for Cu, respectively.

(denotes $4b$ site) and Fe2 (denotes $4c$ site) atoms are associated with the octahedral coordination with different average bond lengths.[2] Thus, the two Fe atoms adopt different topologies of density of states profiles. This implied that the different valence and/or charge states can be expected for the two different Fe atoms in these phases. After self-consistency was achieved, however, the two crystallographically independent Fe atoms possess analogous electronic configuration, which indicates that the degree of charge disproportionation is considerable small. The magnetic moments are 3.85 and 3.10μ_B for Fe1 and Fe2 atom, respectively. Combined with the magnetic moment at the Cu site, $-0.7\mu_B$, and the residual moment residing at the O sites give rise to the total magnetization of 13.0μ_B, which is larger than the experimental saturation magnetization of 9.7μ_B/f.u. The origin of the deviation may be associated with the antisite disorder in the lattice. A significant issue that should be pointed out is that the density of states of Fe2 and O atoms are energetically degenerate and present the similar features, indicating the strong covalent hybridization interactions. This consideration shows that the states corresponding to Fe2 should be d^5L^2 electronic configuration rather than the d^3 configuration, which is in excellent agreement with the small difference of the magnetic moments, and similar electronic configuration among the two crystallographically independent Fe ions and the finite induced magnetic moment on the O site. Experimentally, in order to validate our theoretical conclusion for the charge disproportionation model $2d^5L \rightarrow d^5L^2 + d^5$, it is essential to investigate $CaCu_3Fe_4O_{12}$ by using photoemission spectroscopy and soft x-ray absorption spectroscopy, which can provide valuable information on the valence states and electronic structures.

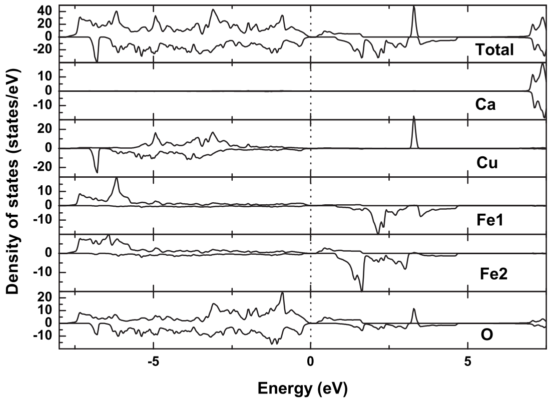

FIG. 4. The total and site-decomposed electronic density of states for ferrimagnetic configuration for low-temperature Pn-3 phase $CaCu_3Fe_4O_{12}$ obtained by GGA+U within U=4.0 eV for Fe and U=7.0 eV for Cu, respectively.

In order to gain more insight into the charge disproportionation and assess its effect on the electronic properties, we briefly compare the total electron charges and the $3d$ charges inside the atomic sphere of Fe1 and Fe2 cations. Due to the strong screening effect of O $2p$-Fe $3d$ e_g σ-type bonds, the difference is small (0.05e/0.03e), as presented in Fig. 2. This variation is the same order as that of Ni ions in $YNiO_3$ and $NdNiO_3$.[15] This clearly demonstrates that the degree of charge disproportionation is rather low, which may give a hint why the magnetic moment at the Fe1 site is slightly larger than that at the Fe2 site. On the other hand, it again evidences that the Fe2 has covalent electronic state that can be expressed as d^5L^2, where L denotes a ligand hole. In order to explore whether there exists a hole character within the oxygen sites, we have also checked the total p occupation from the occupation matrix. All the p states are occupied with an occupation number of 0.60, irrespective of the majority/minority spin states. The orbital occupation values clearly show the existence of substantial hole in the O $2p$ shell of $CaCu_3Fe_4O_{12}$.

According to the presented scenario, $CaCu_3Fe_4O_{12}$ should be considered as a charge disproportionation insulator with a small charge-transfer gap rather than a homogeneous valence and orbital degenerate half-metal. Furthermore, we add a comment on the effects of strong electron correlation in $CaCu_3Fe_4O_{12}$. GGA predicts $CaCu_3Fe_4O_{12}$ to be metallic within the low-temperature phase, in contrast to the experimental observations. Apparently, the electron-electron correlations, mainly in the $3d$ shell of Fe cations, play a significant role. Therefore, we conclude that the charge disproportionation is mainly due to the large contribution of the oxygen holes via the strong covalent hybridization interactions (as evidenced from Fig. 4) in this case instead of the strong reduction in the effective Coulomb potential U as the delocalization of the e_g electrons, as speculated for $LuNiO_3$.[1] The reason for this contradiction is associated with the fact that almost all holes are on oxygen sites in this case. This leads to the minimal reduction in the Hubbard U at the Fe sites. One should expect that the charge disproportionation is coupled with the lattice distortion, where the smaller oxygen octahedron is surrounding the Fe2 site and stabilizes the low-temperature phase of $CaCu_3Fe_4O_{12}$.

In conclusion, extensive *ab initio* calculations have been performed for the two different phases (high temperature/low temperature) of $CaCu_3Fe_4O_{12}$, focusing on the electronic structure and valence states of the Fe ions. Our results indicated that the ground state of $CaCu_3Fe_4O_{12}$ should be considered as a charge disproportionation $(Fe^{(4-\delta)+}/Fe^{(4+\delta)+})$ insulator with a small charge-transfer gap rather than a homogeneous valence (Fe^{4+}) and orbital degenerate half-metal. The charge disproportionation is of $2d^5L \rightarrow d^5L^2 + d^5$ type, not $2d^4 \rightarrow d^3 + d^5$ type, and the origin for this phenomenon is driven primarily by the large contribution of the oxygen holes via the strong covalent hybridization interactions between the Fe d and O p states.

The authors wish to express thanks to D. I. Khomskii for fruitful discussions and critical reading of the manuscript. This work was supported through the financial support from the National Natural Science Foundation of China for Grants No. 20671088, No. 20661026 20871023, and No. 20831004.

---

*Corresponding author. FAX: +86-431-85698041. xfhao1980@yahoo.com.cn

†jmeng@ciac.jl.cn

[1] I. I. Mazin, D. I. Khomskii, R. Lengsdorf, J. A. Alonso, W. G. Marshall, R. M. Ibberson, A. Podlesnyak, M. J. Martínez-Lope, and M. M. Abd-Elmeguid, Phys. Rev. Lett. **98**, 176406 (2007); T. Mizokawa, D. I. Khomskii, and G. A. Sawatzky, Phys. Rev. B **61**, 11263 (2000).

[2] I. Yamada, K. Takata, N. Hayashi, S. Shinohara, M. Azuma, S. Mori, S. Muranaka, Y. Shimakawa, and M. Takano, Angew. Chem., Int. Ed. **47**, 7032 (2008).

[3] A. E. Bocquet, A. Fujimori, T. Mizokawa, T. Saitoh, H. Namatame, S. Suga, N. Kimizuka, Y. Takeda, and M. Takano, Phys. Rev. B **45**, 1561 (1992); T. Akao, Y. Azuma, M. Usuda, Y. Nishihata, J. Mizuki, N. Hamada, N. Hayashi, T. Terashima, and M. Takano, Phys. Rev. Lett. **91**, 156405 (2003).

[4] T. Mizokawa, H. Namatame, A. Fujimori, K. Akeyama, H. Kondoh, H. Kuroda, and N. Kosugi, Phys. Rev. Lett. **67**, 1638 (1991).

[5] E. Sjöstedt, L. Nordström, and D. J. Singh, Solid State Commun. **114**, 15 (2000).

[6] G. K. H. Madsen, P. Blaha, K. Schwarz, E. Sjöstedt, and L. Nordström, Phys. Rev. B **64**, 195134 (2001).

[7] K. Schwarz and P. Blaha, Comput. Mater. Sci. **28**, 259 (2003).

[8] P. Blaha, K. Schwarz, G. K. H. Madsen, D. Kvasnicka, and J. Luitz, *WIEN2k, An Augmented Plane Wave Plus Local Orbitals Program for Calculating Crystal Properties* (Vienna University of Technology, Austria, 2001).

[9] P. E. Blöchl, Phys. Rev. B **50**, 17953 (1994).

[10] J. P. Perdew, K. Burke, and M. Ernzerhof, Phys. Rev. Lett. **77**, 3865 (1996).

[11] A. I. Liechtenstein, V. I. Anisimov, and J. Zaanen, Phys. Rev. B **52**, R5467 (1995).

[12] V. Anisimov, F. Aryasetiawan, and A. Lichtenstein, J. Phys.: Condens. Matter **9**, 767 (1997).

[13] A. G. Petukhov, I. I. Mazin, L. Chioncel, and A. I. Lichtenstein, Phys. Rev. B **67**, 153106 (2003).

[14] H. P. Xiang, X. J. Liu, E. J. Zhao, J. Meng, and Z. J. Wu, Appl. Phys. Lett. **91**, 011903 (2007).

[15] S. Yamamoto and T. Fujiwara, J. Phys. Soc. Jpn. **71**, 1226 (2002).